Organometallic Chemistry | *Very Important Paper*

VIP Terminal Alkyne Coupling Reactions Through a Ring: Effect of Ring Size on Rate and Regioselectivity

Caroline M. Storey, Matthew R. Gyton, Rhiann E. Andrew, and Adrian B. Chaplin*[a]

Abstract: Terminal alkyne coupling reactions promoted by rhodium(I) complexes of macrocyclic NHC-based pincer ligands—which feature dodecamethylene, tetradecamethylene or hexadecamethylene wingtip linkers *viz.* [Rh(CNC-n)(C_2H_4)][BAr^F_4] (n = 12, 14, 16; Ar^F = 3,5-$(CF_3)_2C_6H_3$)—have been investigated, using the bulky alkynes HC≡C*t*Bu and HC≡CAr′ (Ar′ = 3,5-$tBu_2C_6H_3$) as substrates. These stoichiometric reactions proceed with formation of rhodium(III) alkynyl alkenyl derivatives and produce rhodium(I) complexes of conjugated 1,3-enynes by C–C bond reductive elimination through the annulus of the ancillary ligand. The intermediates are formed with orthogonal regioselectivity, with *E*-alkenyl complexes derived from HC≡C*t*Bu and *gem*-alkenyl complexes derived from HC≡CAr′, and the reductive elimination step is appreciably affected by the ring size of the macrocycle. For the homocoupling of HC≡C*t*Bu, *E*-*t*BuC≡CCH=CH*t*Bu is produced via direct reductive elimination from the corresponding rhodium(III) alkynyl *E*-alkenyl derivatives with increasing efficacy as the ring is expanded. In contrast, direct reductive elimination of Ar′C≡CC(=CH_2)Ar′ is encumbered relative to head-to-head coupling of HC≡CAr′ and it is only with the largest macrocyclic ligand studied that the two processes are competitive. These results showcase how macrocyclic ligands can be used to interrogate the mechanism and tune the outcome of terminal alkyne coupling reactions, and are discussed with reference to catalytic reactions mediated by the acyclic homologue [Rh(CNC-Me)(C_2H_4)][BAr^F_4] and solvent effects.

Introduction

Intermolecular carbon-carbon bond forming reactions are amongst the most coveted disconnections in synthetic organic chemistry. As a conceptually straightforward and atom economical method for the preparation of conjugated 1,3-enynes, the transition metal catalysed dimerisation of terminal alkynes is an example of growing importance.[1,2] These enynes are versatile unsaturated synthons and key subunits of biologically active compounds and functional materials, however, their selective formation remains difficult to realise. In addition to competing metal-catalysed reactions of terminal alkynes, that can lead to a range of alternative unsaturated products,[3,4] the formal addition of the C(sp)–H bond of one alkyne across the C≡C bond of another is a process that can result in three different 1,3-enyne isomers by virtue of head-to-tail (*gem*-) or head-to-head coupling (*E*- and *Z*-) as depicted in Scheme 1.[1] Indeed, although a wide variety of catalysts—based on transition metals, lanthanides, actinides, and main group elements—have been shown to promote these reactions, few are capable of producing single enyne isomers with high fidelity; the majority lead to mixtures of regio- or stereo- isomers.[1] Greater mechanistic understanding of these reactions is therefore required to enable rational design of more effective catalysts

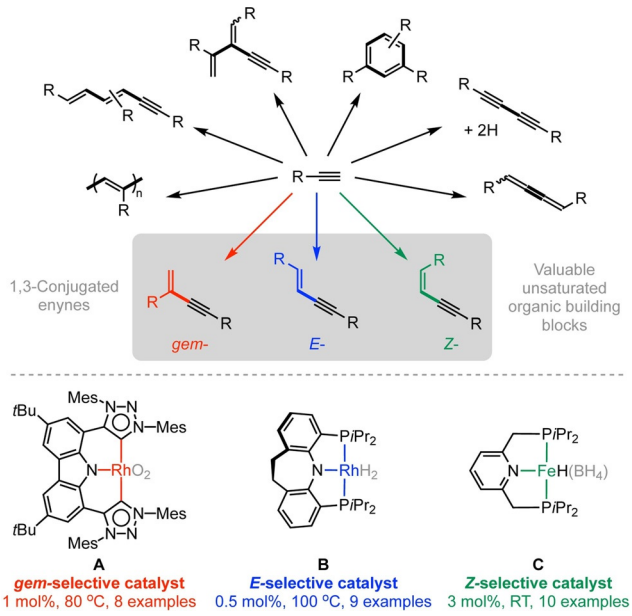

Scheme 1. Metal catalysed reactions of terminal alkynes. Mes = 2,4,6-$Me_3C_6H_2$.

[a] *Dr. C. M. Storey, Dr. M. R. Gyton, Dr. R. E. Andrew, Dr. A. B. Chaplin*
Department of Chemistry, University of Warwick
Gibbet Hill Road, Coventry CV4 7AL (UK)
E-mail: a.b.chaplin@warwick.ac.uk

Supporting information and the ORCID identification number(s) for the author(s) of this article can be found under: https://doi.org/10.1002/chem.202002962.

and promote further application of terminal alkyne coupling reactions in organic synthesis.

Rigid *mer*-tridentate "pincer" ligands are attractive ancillaries for homogenous catalysis, conferring high thermal stability and supporting a broad range of metal-based reactivity.[5,6] Application of these ligands in transition metal promoted terminal alkyne coupling reactions is of contemporary interest, with examples **A**–**C** showcasing the capacity of this ligand class to enforce high product selectivity.[7,8,9] Along with advances made employing other ancillary ligands,[10,11] a number of rhodium pincers have emerged as state of the art catalysts. Mesoionic carbene-based Rh(CNC) complex **A**, for instance, is noteworthy for the efficient *gem*-selective homocoupling of terminal alkynes (1 mol%, 80 °C).[7] Using this precatalyst, 1-hexyne and a series of heteroatom functionalised alkyl alkynes were converted exclusively to the corresponding *gem*-enynes, while a mixture of *gem*- (89%) and *E*- (11%) products was obtained with phenyl acetylene. Conversely, phosphine-based Rh(PNP) complex **B** principally afforded *E*-enyne products (>90%) under similar conditions (0.5 mol%, 100 °C) for a range of alkyl and aryl alkynes, although *tert*-butyl acetylene was notably associated with lower fidelity for this isomer (58%).[8] Closely related Rh(PNP) and Rh(PCP) catalysts demonstrate reduced selectivity, giving mixtures composed predominately of *gem*- and *E*-products.[8,12] Recently a range of Fe(PNP) complexes have been shown to promote *Z*-selective homocoupling reactions, with **C** the formative example.[9,13]

Commonly accepted mechanisms for the formation of enynes from terminal alkynes typically invoke distinct pathways involving either alkyne insertion into a M–H bond ("hydrometallation"), alkyne insertion into a M–C bond ("carbometallation"), or formation of a metal vinylidene intermediate ("vinylidene").[1] Head-to-tail coupling of alkynes can be accounted for using the first two scenarios, while the third is required to reconcile the formation of *Z*-isomers. In the context of homocoupling reactions promoted by rhodium pincer complexes such as **A** and **B**, where reactive three-coordinate rhodium(I) 14 VE species are inferred as the active catalysts, the hydrometallation pathways depicted in Scheme 2 are most likely operative.[12] Both involve initial C(sp)–H bond oxidative addition, but bifurcate on coordination of the second alkyne to afford the *gem*- or *E*- regioisomers. This assertion is supported by the absence of *Z*-enyne products, organometallic chemistry of related rhodium complexes,[4,11] and stoichiometric alkyne dimerisation reactions of an Ir(PCP) pincer complex.[14] Formation of rhodium vinylidene complexes from the reaction between rhodium(I) precursors and terminal alkynes is, however, not uncommon suggesting that a vinylidene mechanism (Scheme 2) should not be discounted without experimental evidence to the contrary.[15]

As part of our work investigating the organometallic chemistry of NHC-based pincer complexes,[16,17,18] we have previously shown that [Rh(CNC-Me)(C_2H_4)][BAr^F_4] (**1-Me**, Ar^F = 3,5-(CF_3)$_2C_6H_3$; Scheme 3) catalyses the homocoupling of HC≡C*t*Bu and HC≡CAr′ (Ar′ = 3,5-*t*Bu$_2C_6H_3$) with orthogonal regioselectivity: proceeding with exclusive formation of *E*-enyne and *gem*-enyne products, respectively.[19,20] The regioselectivity of the

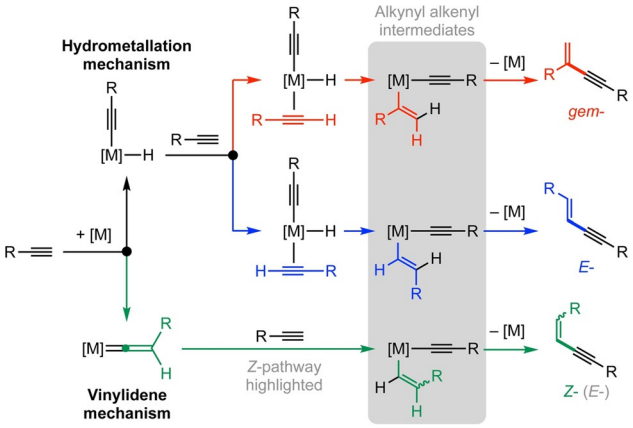

Scheme 2. Selected pathways for the catalytic homocoupling of terminal alkynes into 1,3-conjugated enynes.

latter is remarkably reversed with the macrocyclic variant **1-12**. The stoichiometric C–C bond coupling occurring through the annulus of the ancillary ligand, where the head-to-head product *E*-Ar′C≡CCH=CHAr′ becomes mechanically entrapped. Following communication of this initial finding,[19] we now detail a systematic exploration of the capacity of macrocyclic CNC ligands to impart reaction control of terminal alkyne coupling reactions: using HC≡C*t*Bu and HC≡CAr′ as substrates, and macrocyclic ligands with different ring sizes, *viz.* [Rh(CNC-n)(C_2H_4)][BAr^F_4] (**1-n**, n = 12, 14, 16; Scheme 3).

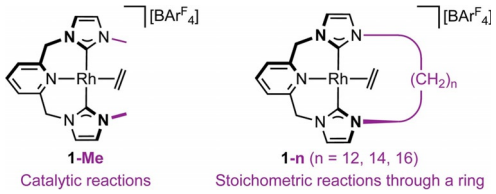

Scheme 3. Rh(CNC) pincers **1-Me** and **1-n** (n = 12, 14, 16).

Results and discussion

Substrate and solvent dependence of homocoupling reactions promoted by 1-12

As a starting point, reactions between **1-12** (20 mmolL^{-1}) and the terminal alkynes (2.1 equiv) were studied *in situ* using the weakly coordinating solvents CD_2Cl_2 and 1,2-difluorobenzene (DFB) at RT.[21] Quantitative spectroscopic conversion to rhodium(III) alkynyl alkenyl derivatives ***E*-2-12** and ***gem*-3-12** was observed for HC≡C*t*Bu and HC≡CAr′, respectively, within 5 min (Figure 1). Formation of these complexes can be reconciled by a common hydrometallation mechanism and the orthogonal regioselectivity is consistent with that observed in the corresponding homocoupling reactions catalysed by **1-Me**: it is therefore ascribed to the electronic and steric characteristics of the Rh(CNC) core alone.[20] The presence of the dodecamethylene wingtip linker, however, attenuates onward product

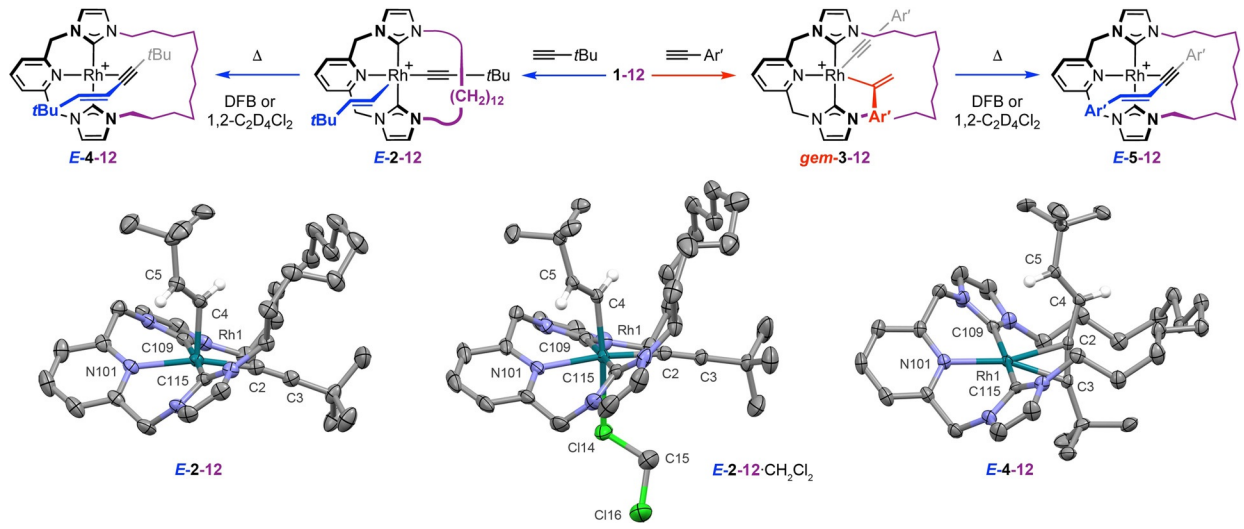

Figure 1. Reactions of **1-12** with HC≡C*t*Bu and HC≡CAr′. Solid-state structures of ***E*-2-12**, ***E*-2-12**·CH_2Cl_2 and ***E*-4-12**: thermal ellipsoids drawn at 50%, 30% and 50% probability, respectively; anions, solvent molecules, and most hydrogen atoms omitted for clarity. Selected bond lengths (Å) and angles (deg): ***E*-2-12**: Rh1-C2, 1.958(3); C2-C3, 1.208(4); Rh1-C2-C3, 169.2(2); Rh1-C4, 1.995(2); C4-C5, 1.322(4); Rh1-C4-C5, 126.3(2); Rh1-N101, 2.174(2); Rh1-C109, 2.090(2); Rh1-C115, 2.018(2); N101-Rh1-C2, 167.27(9); ***E*-2-12**·CH_2Cl_2: Rh1-C2, 1.978(4); C2-C3, 1.204(6); Rh1-C2-C3, 171.0(4); Rh1-C4, 2.003(4); C4-C5, 1.324(6); Rh1-C4-C5, 125.0(3); Rh1-Cl14, 2.7027(13); Rh1-N101, 2.182(4); Rh1-C109, 2.103(5); Rh1-C115, 2.038(5); N101-Rh1-C2, 171.9(2); ***E*-4-12**: Rh1-Cnt(C2,C3), 2.019(3); C2-C3, 1.243(6); C2-C4, 1.452(5); C4-C5, 1.333(5); C2-C4-C5, 122.1(3); Rh1-N101, 2.103(3); Rh1-C109, 2.071(3); Rh1-C115, 2.038(3); N101-Rh1-Cnt(C2,C3), 178.37(12); py-Rh-C≡C twist, 31.9(2).

forming C–C bond reductive elimination and both aforementioned rhodium(III) derivatives are sufficiently persistent at RT to be isolated in high yield on a larger scale. The former, ***E*-2-12** was obtained as an authentically five-coordinate complex by recrystallisation from DFB solution (93% yield) and the corresponding dichloromethane adduct ***E*-2-12**·CH_2Cl_2 when this more coordinating solvent was used (73% yield, Figure 1). Previously ***gem*-3-12** was isolated from CH_2Cl_2 solution in 47% yield,[19] but a higher yield can be obtained when DFB is employed (73%).

The structure of ***E*-2-12** in the solid state is notable for the adoption of a square-pyramidal coordination geometry, with the *E*-alkenyl in the apical position and the alkynyl *trans* to the pyridyl donor. This configuration is also observed for ***E*-2-12**·CH_2Cl_2, but interaction with dichloromethane confers an 18 VE configuration; the associated Rh1-Cl14 contact (2.7027(13) Å) is in line with known rhodium(III) precedents (2.49–2.76 Å).[16,22] Solvent coordination is associated with slight elongation of the metal-ligand bonds as expected for the change in metal coordination geometry, with perturbation of the alkynyl Rh1–C2 bond [1.978(4) *cf.* 1.958(3) Å] the most notable, and straightening of the N101-Rh1-C2 angle [171.9(2) *cf.* 167.27(9)°]. In the case of previously reported ***gem*-3-12**, it is the alkynyl which is found in the apical position [Rh1-C2, 2.939(6) Å], with the *gem*-alkenyl located *trans* to the pyridyl donor [Rh1-C4, 1.983(5) Å, *cf.* 1.995(2)/2.003(4) Å for ***E*-2-12**/***E*-2-12**·CH_2Cl_2], enabling adoption of a π-interaction with the Ar′ substituent [Rh1-Cnt(C=C), 2.467(4) Å] and conferring an 18 VE configuration.[19] Crystallographically characterised rhodium(III) alkynyl alkenyl precedents are limited to a single coordinatively saturated example featuring a dienyl ligand [Rh-C≡C, 1.937(8); Rh-C=C, 2.015(9) Å].[4]

In CD_2Cl_2 solution at 298 K, the coupled ^{1}H resonances of the *E*-alkenyl in ***E*-2-12** can be observed at δ 6.53 (RhCH=CH) and 3.55 (RhCH=CH). The magnitude of the coupling constant ($^3J_{HH}$ = 13.5 Hz) is consistent with the structural formulation as are the characteristics of the associated ^{13}C resonances, which are located at δ 119.7 (RhCH=CH) and 144.3 (RhCH=CH); the former exhibiting appreciable coupling to ^{103}Rh ($^1J_{RhC}$ = 37 Hz). The alkynyl ^{13}C signals can also be identified at δ 120.0 (RhC≡C, $^2J_{RhC}$ = 12 Hz) and 82.8 (RhC≡C, $^1J_{RhC}$ = 57 Hz). The ^{1}H NMR spectrum at this temperature is noteworthy for higher than expected symmetry and extensive line broadening of the pyCH_2 and NCH_2 resonances, indicating rapid atropisomerism of the pincer backbone on the NMR timescale (500 MHz). This process was qualitatively probed by variable temperature ^{1}H NMR spectroscopy, with the C_1 symmetric slow exchange regime reached upon cooling to 225 K (see ESI). Similar structural dynamics were observed for ***gem*-3-12** in CD_2Cl_2 solution, but the *gem*-alkenyl [δ_{1H} 5.57, 5.76; δ_{13C} 157.7 (RhC=CH_2, $^1J_{RhC}$ = 27 Hz), 114.6 (RhC=CH_2)] and alkynyl [δ_{13C} 104.7 (RhC≡C, $^2J_{RhC}$ = 15 Hz), 85.0 (RhC≡C, $^1J_{RhC}$ = 72 Hz)] ligands can be readily identified by NMR spectroscopy.[19] Cooling ***gem*-3-12** to 225 K resulted in decoalescence of the pincer ^{1}H resonances and, consistent with π-coordination of the alkenyl Ar′ substituent, one set of the 3,5-*t*Bu$_2$C$_6$H$_3$ signals (500 MHz). These data fully corroborate the structures of ***E*-2-12** and ***gem*-3-12** observed in the solid state, with the magnitudes of the $^1J_{RhC}$ coupling constants consistent with the different σ-organyl configurations. Similar spectroscopic signatures are observed in DFB solution.

Heating ***E*-2-12** in 1,2-$C_2D_4Cl_2$ or DFB solution (20 mmolL^{-1}) resulted in C–C bond reductive elimination through the annulus of the bound CNC-12 ligand and formation of the corresponding *E*-enyne complex ***E*-4-12**, completing the formal

Table 1. Activation parameters for C–C bond reductive elimination reactions.

Reaction	Solvent	$\Delta H^{\ddagger}$ [kJ mol^{-1}]	$\Delta S^{\ddagger}$ [J K^{-1} mol^{-1}]	$\Delta G^{\ddagger}_{298K}$ [kJ mol^{-1}]	$t_{1/2}$ (328 K)
***E*-2-12→*E*-4-12**	1,2-$C_2D_4Cl_2$	125 ± 1	+55 ± 4	109 ± 3	210 min
***E*-2-12→*E*-4-12**	DFB	93 ± 1	−24 ± 4	101 ± 5	22 min
***gem*-3-12→*E*-5-12**[a]	1,2-$C_2D_4Cl_2$	119 ± 1	+44 ± 4	106 ± 3	92 min
***gem*-3-12→*E*-5-12**	DFB	109 ± 3	+8 ± 9	106 ± 6	125 min
***gem*-3-Me→*gem*-5-Me**[a]	CD_2Cl_2	97 ± 1	+15 ± 5	93 ± 3	51 s[b]
***gem*-3-Me→*gem*-5-Me**[c]	DFB	95 ± 3	+28 ± 10	87 ± 6	5 s[b]

[a] From ref. [19]. [b] Extrapolated using the activation parameters. [c] Determined as part of this work for comparison.

head-to-head coupling of HC≡C*t*Bu [$t_{1/2}$(328 K) = 210 min, 1,2-$C_2D_4Cl_2$; 22 min, DFB]. This reaction was followed *in situ* by ^{1}H NMR spectroscopy and found to follow first order kinetics across a wide temperature range (328–348 K, 1,2-$C_2D_4Cl_2$; 313–333 K, DFB). The associated activation parameters were determined by Eyring analysis and highlight a large solvent dependence. The reaction is characterised by a 32 kJ mol^{-1} higher activation enthalpy and positive activation entropy, when carried out in 1,2-$C_2D_4Cl_2$ compared to DFB ($\Delta\Delta S^{\ddagger} = +79$ J K^{-1} mol^{-1}, Table 1). These differences are fully consistent with appreciable coordination of the chlorocarbon solvent to ***E*-2-12**: an interpretation in line with the relative donor ability and explicitly evidenced by isolation of ***E*-2-12**·CH_2Cl_2 (*vide supra*). The product ***E*-4-12** was isolated in 85% yield and fully characterised in solution and the solid state (Figure 1 and *vide infra*).

We have previously communicated that thermolysis of ***gem*-3-12** in 1,2-$C_2D_4Cl_2$ does not yield the *gem*-enyne complex ***gem*-5-12** expected for a single reaction step and through extrapolation of the reactivity established for **1-Me**: instead the mechanically interlocked *E*-enyne complex ***E*-5-12** is produced.[19] The same outcome was observed when this reaction was reanalysed in DFB, proceeding with first order kinetics on a similar timescale [20 mmol L^{-1}; $t_{1/2}$(328 K) = 92 min, 1,2-$C_2D_4Cl_2$; 125 min, DFB; Table 1]. A multistep mechanism, starting with β-H abstraction and terminating with C–C bond reductive elimination from ***E*-3-12**, is proposed to reconcile the formation ***E*-5-12** from ***gem*-3-12** and a similar sequence has been established for the stoichiometric homocoupling of HC≡CPh into *E*-PhC≡CCH=CHPh by an Ir(PCP) complex.[14] The proposition is also supported experimentally by isotope labelling experiments, which involved heating ***gem*-3-12** in 1,2-$C_2D_4Cl_2$ or DFB in the presence of excess DC≡CAr′ and resulted in significant deuterium incorporation into both positions of the enyne core. For comparison, no significant isotope scrambling was observed when a 1:1 mixture of ***E*-2-12** and the d_2-isotopologue [Rh(CNC-12)(C≡C*t*Bu)(*E*-CD=CD*t*Bu)][BAr^F_4] was heated in 1,2-$C_2D_4Cl_2$ or DFB, indicating that formation of ***E*-2-12** (from **1-12** and HC≡C*t*Bu) is irreversible with respect to its onward reactivity.[23] On this basis—along with the small solvent dependence—we (now) ascribe formation of ***E*-3-12** by 1,2-migratory insertion as the rate-determining step for ***gem*-3-12→*E*-5-12**; rather than reductive elimination from ***E*-3-12**.[24] The turnover-limiting step in the homocoupling of HC≡CAr′ into Ar′C≡CC(=CH_2)Ar′ catalysed by **1-Me** is associated with C–C bond formation, *viz.* ***gem*-3-Me→*gem*-5-Me**. By reference to the associated activation parameters we conclude that incorporation of the dodecamethylene wingtip linker destabilises direct reductive elimination from ***gem*-3-12** by at least $\Delta G^{\ddagger}_{298K} = 13$ kJ mol^{-1}: presumably a direct consequence of pronounced steric buttressing between the bulky α-aryl substituted alkenyl ligand and the wingtip linker.

Larger macrocyclic proligands and their rhodium complexes

To interrogate the impact of the methylene chain on the rate and regioselectivity of terminal alkyne homocoupling reactions, attention turned to the organometallic chemistry of rhodium complexes of larger macrocyclic CNC ligands. To this end, the new proligands CNC-14·2 HBr and CNC-16·2 HBr were prepared using high dilution versions of procedures developed in our lab for the synthesis of CNC-n·2 HBr (n = 8, 10, 12).[18] Formation of these hygroscopic bis(imidazolium) macrocycles was confirmed in solution through a combination of NMR spectroscopy and ESI-MS. The latter notably enabled alternative formulation as higher order oligomers to be discounted, where [*M*-Br]$^+$ ion peaks with the expected integer isotope pattern were observed [n = 14, 514.2557 (calcd 514.2540); 16, 542.2848 (calcd 542.2853) *m/z*]. As further structural corroboration, neutral imidazole-2-thione and cationic palladium(II) chloride derivatives of both new proligands were prepared enabling construction of homologous series of the form CNC-Me·S_2 and CNC-n·S_2 (n = 12, 14, 16), and [Pd(CNC-Me)Cl]$^+$ (**6-Me**)[25] and [Pd(CNC-n)Cl]$^+$ (**6-n**; n = 8, 10, 12,[18] 14, 16): full details are provided in the ESI.

Using an analogous three-step copper transmetalation procedure to that described for **1-Me** and **1-12**,[19] the rhodium ethylene derivatives **1-14** (78%) and **1-16** (67%) were isolated as analytically pure materials in good overall yield and fully characterised (Figure 2). These complexes are extremely air-sensitive, but can be stored for prolonged periods in the solid state under an inert atmosphere without appreciable decomposition. As for the other Rh(CNC) congeners, **1-14** and **1-16** are appreciably fluxional in CD_2Cl_2 solution at ambient temperature, exhibiting broadened py$C\underline{H}_2$, N$C\underline{H}_2$ and $C_2\underline{H}_4$ signals consistent with atropisomerism of the pincer backbone on the ^{1}H NMR timescale (500 MHz). The ^{13}C resonance of coordinated ethylene can be located at *ca.* δ 50 by HSQC experiments for **1-14** and **1-16** in agreement with that observed for **1-12** (δ 47), but noting this signal could not be located for **1-Me**.[19] The carbene resonances for **1** range from δ 181.9–184.8, in-

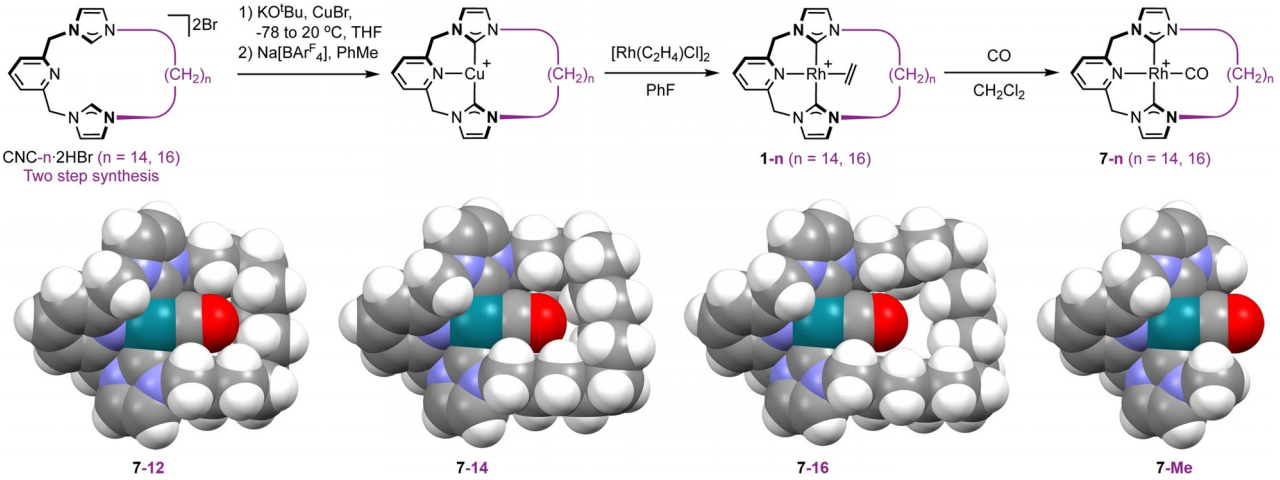

Figure 2. Synthesis of rhodium(I) complexes of CNC-14 and CNC-16. Solid-state structures of **7-12**,[19] **7-14**, **7-16**, and **7-Me**[19] in spacefill format: only one unique cation is shown for **7-14** and **7-16** ($Z'=2$). Anions and minor disordered components (methylene chain in **7-14**) omitted for clarity.

creasing in the order **1-12** < **1-14** < **1-16** < **1-Me**, consistent with that observed for **6**, and are strongly coupled to ^{103}Rh ($^1J_{RhC}$ = 40–41 Hz).

The donor properties of the CNC ligands have been assessed systematically using rhodium carbonyl derivatives [Rh(CNC-Me)(CO)][BAr$^F_4$] (**7-Me**) and [Rh(CNC-n)(CO)][BAr$^F_4$] (**7-n**; n = 12, 14, 16), exploiting the ν(CO) stretching band as a convenient spectroscopic handle (Table 2).[26] These carbonyl complexes were obtained in quantitative spectroscopic yield by reaction of **1** with carbon monoxide and the complete series has been characterised in the solid state by X-ray diffraction. The IR data of **7** in CH_2Cl_2 solution indicate the net donor strengths are equivalent within error (Table 2) and this interpretation is reinforced by location of all the ^{13}C carbonyl resonances at δ 194 with $^1J_{RhC}$ = 80 Hz (CD_2Cl_2). Pertinent to the onward reactivity of **1-n**, inspection of the space-filling diagrams and observation of solution phase C_2 confirms the carbonyl ligand is readily accommodated within the cavity defined by the tethered wingtip substituents (Figure 2).

Table 2. Carbonyl stretching frequencies of **7** (CH_2Cl_2).

	ν(CO) [cm^{-1}]	Source
7-12	1978	ref. [19]
7-14	1978	this work
7-16	1978	this work
7-Me	1980	ref. [19]

Effect of increasing the ring size on the homocoupling of HC≡C*t*Bu

With the new rhodium ethylene precursors in hand, the effect of increasing the ring size was first investigated for the homocoupling of HC≡C*t*Bu in DFB. Reactions of **1-14** and **1-16** (20 mmolL^{-1}) with HC≡C*t*Bu (5 equiv) were monitored *in situ* by NMR spectroscopy at RT, revealing quantitative spectroscopic conversion to the corresponding rhodium(I) *E*-enyne complexes ***E*-4-14** and ***E*-4-16** within 2 h; with the latter considerably faster than the former (Figure 3). The products were subsequently isolated in excellent yield on a larger scale (81 and 94%, respectively) and extensively characterised in solution and the solid state.

In CD_2Cl_2 solution the three new *E*-enyne complexes ***E*-4-n** (n = 12, 14, 16) are characterised by C_1 symmetry, downfield shifted *E*-alkene ^{1}H resonances (CH=C<u>H</u>*t*Bu, δ 6.60–7.44, *cf.* 6.05; C<u>H</u>=CH*t*Bu, δ 6.00–6.05, *cf.* 5.39) with $^3J_{HH}$ = 15 Hz and ^{103}Rh coupled alkyne ^{13}C resonances (C≡<u>C</u>*t*Bu, δ 89.5–95.4, $^1J_{RhC}$ = 14–16 Hz; <u>C</u>≡C*t*Bu, δ 72.8–75.6, $^1J_{RhC}$ = 10–12 Hz). These data are fully consistent with the structural formulations, in agreement with those previously reported for ***E*-4-Me**,[20] and supported by elucidation in the solid state by single crystal X-ray diffraction (Figures 1 and 3). The solid-state structures of ***E*-4-n** unequivocally evidence the interpenetrated coordination mode of the enyne, which is bound to the metal with contacts of 2.019(3), 2.040(14) and 2.019(2) Å, for n = 12, 14, 16 respectively; marginally elongated compared with ***E*-4-Me** [2.006(3) Å].[20]

Analysis of reactions of **1-14** and **1-16** with HC≡C*t*Bu in DFB at 278 K *in situ* by NMR spectroscopy enabled ***E*-2-14** and ***E*-2-16** to be established as intermediates in the formation of ***E*-4-14** and ***E*-4-16**, respectively, with β-alkenyl ^{1}H signals the most diagnostic (***E*-4-14**, δ 3.61, $^3J_{HH}$ = 12.1 Hz; ***E*-4-16**, δ 3.63, $^3J_{HH}$ = 12.1 Hz; *cf.* ***E*-4-12** at 298 K, δ 3.65, $^3J_{HH}$ = 12.6 Hz). Conversion to the rhodium(III) intermediates is fast relative to the onward formation of the corresponding *E*-enyne complex and the determination of the associated rates enable increasingly facile C–C bond reductive elimination to be quantified at 278 K in the order ***E*-2-16** ($t_{1/2}$ = 33 min) > ***E*-2-14** ($t_{1/2}$ = 280 min) > > ***E*-2-12** ($t_{1/2}$ > 9 days). Having established that the donor properties of CNC-n are equivalent, electronic explanations can be ruled out and instead we attribute the increase in rate to reduced intercalation of the methylene chain between the approaching σ-organyls: steric buttressing that would hinder adoption of the distorted trigonal bipyramidal transition state geometry required for C–C bond reductive elimination.

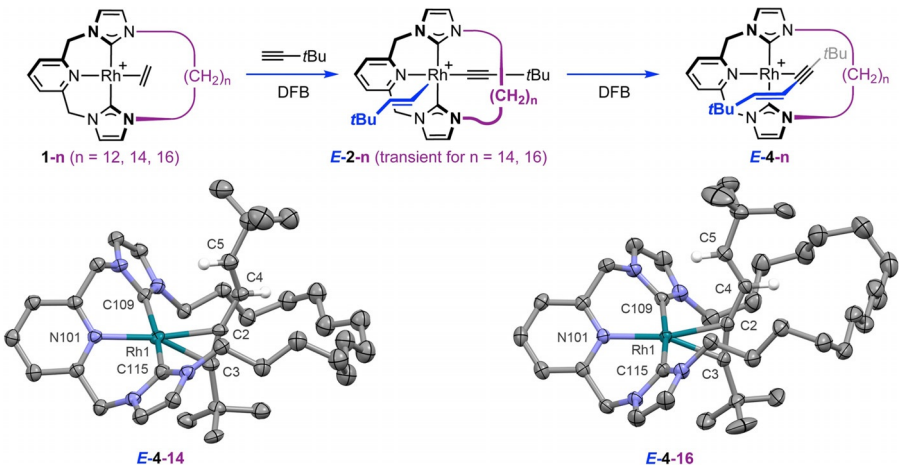

Figure 3. Reactions of **1-n** with HC≡C*t*Bu. Solid-state structures of ***E*-4-14** and ***E*-4-16**: thermal ellipsoids drawn at 30% and 50% probability, respectively; anions, solvent molecules, and most hydrogen atoms omitted for clarity. Selected bond lengths (Å) and angles (deg): ***E*-4-14**: Rh1-Cnt(C2,C3), 2.040(14); C2-C3, 1.22(2); C2-C4, 1.38(2); C4-C5, 1.31(2); C2-C4-C5, 128(2); Rh1-N101, 2.119(13); Rh1-C109, 2.07(2); Rh1-C115, 2.01(2); N101-Rh1-Cnt(C2,C3), 170.7(6); py-Rh-C≡C twist, 28.0(12); ***E*-4-16**: Rh1-Cnt(C2,C3), 2.019(2); C2-C3, 1.245(3); C2-C4, 1.441(3); C4-C5, 1.323(3); C2-C4-C5, 123.5(2); Rh1-N101, 2.107(2); Rh1-C109, 2.060(2); Rh1-C115, 2.016(2); N101-Rh1-Cnt(C2,C3), 175.67(7); py-Rh-C≡C twist, 31.96(15).

Effect of increasing the ring size on the homocoupling of HC≡CAr′

On turning to reactions of **1-14** and **1-16** with a twofold excess of HC≡CAr′ in DFB, it quickly became apparent from analysis *in situ* by NMR spectroscopy that rhodium(III) alkynyl alkenyl derivatives ***gem*-3-14** and ***gem*-3-16** are formed rapidly, in quantitative spectroscopic yield, and are considerably more thermally robust than ***gem*-3-12**. Both new complexes were subsequently isolated in excellent yield on a larger scale (73 and 90%, respectively) and extensively characterised, including ***gem*-3-16** in the solid state by single crystal X-ray diffraction (Figure 4).

As for the dodecamethylene variant, ***gem*-3-14** and ***gem*-3-16** are structurally fluxional in CD_2Cl_2 solution at 298 K, exhibiting very broad pincer ^{1}H resonances consistent with rapid atropisomerism of the ancillary ligand on the NMR timescale (500 MHz). Nevertheless, the *gem*-alkenyl [***gem*-3-14**, δ 5.66, 5.74; ***gem*-3-16**, δ 5.67, 5.70; *cf.* ***gem*-3-12**, δ 5.57, 5.76] and two sharp 18H 3,5-tBu$_2$C$_6$H$_3$ resonances are readily discerned from the ^{1}H NMR spectrum of each complex at this temperature. The structural dynamics of the pincer ligand are arrested upon cooling to 225 K and restricted rotation of one of the Ar′ groups becomes apparent. The latter is consistent with π-coordination of the alkenyl Ar′ substituent observed in the solid for ***gem*-3-12** [Rh1-Cnt(C=C), 2.467(4) Å] and ***gem*-3-16** [Rh1-Cnt(C=C), 2.579(4) Å]. The ^{13}C NMR spectroscopic characteristics of the σ-organyl ligands in ***gem*-3-14** [δ 156.8 (RhC=CH$_2$, $^1J_{RhC}$ = 25 Hz), 114.5 (RhC=CH$_2$), 104.8 (RhC≡C, $^2J_{RhC}$ = 16 Hz), 85.8 (RhC≡C, located by HMBC)] and ***gem*-3-16** [δ 155.6 (RhC=CH$_2$, located by HMBC), 115.3 (RhC=CH$_2$), 105.4 (RhC≡C, $^2J_{RhC}$ = 15 Hz), 87.2 (RhC≡C, located by HMBC)] are fully consistent with their structural formulations and, moreover, congruent with those determined for ***gem*-3-12** [δ 157.7 (RhC=CH$_2$, $^1J_{RhC}$ = 27 Hz), 114.6 (RhC=CH$_2$), 104.7 (RhC≡C, $^2J_{RhC}$ = 15 Hz), 85.0 (RhC≡C, $^1J_{RhC}$ = 72 Hz)]. The key solid-state metrics of ***gem*-3-16** [*e.g.*, Rh1-C2, 1.920(5); Rh1-C4, 1.971(5) Å] are only slightly perturbed from those of ***gem*-3-12** [Rh1-C2, 1.940(5); Rh1-C4, 1.983(5) Å], with the more prominent contraction of the alkenyl contact consistent with reduced π-coordination of the Ar′ substituent (*vide supra*).

Prolonged heating of ***gem*-3-14** and ***gem*-3-16** at elevated temperature was required to induce onward reactivity in DFB. The former proceeded smoothly to afford ***E*-5-14**, with $t_{1/2}$ = 91 min at 353 K and was isolated from solution in 84% yield. This exclusive switch in regioselectivity mirrors that observed for the dodecamethylene variant ($t_{1/2}$ < 10 min at 353 K) but is not maintained for ***gem*-3-16**, where instead a ≈1:1 mixture of ***gem*-5-16** and ***E*-5-16** results at 353 K ($t_{1/2}$ = 66 min). The formation of ***gem*-5-16** indicates that the associated single step C–C bond reductive elimination is competitive with production of *E*-Ar′C≡CCH=CHAr′ within the macrocycle. Successive recrystallisation enabled separation of the two regioisomers of **5-16**, which were obtained as analytically pure materials and extensively characterised; including in the solid state by single crystal X-ray diffraction (Figure 4). As reflected in the reactivity of ***E*-2-n** and on the basis of reduced buttressing with the bulky α-aryl substituted alkenyl ligand, the logical consequence of lengthening of the wingtip linker is a reduced activation barrier for direct C–C bond reductive elimination from ***gem*-3-n** and formation of ***gem*-5-n**, *i.e.*, the reactivity tends toward that of ***gem*-3-Me**. In the homologous series studied, the tipping point is clearly reached for the hexadecamethylene congener, as shown by the reaction *outcome*: the rates for the smaller ring systems instead reflect changes in the activation barrier for the competitive head-to-head coupling process and are clearly nuanced.

The structures of ***E*-5-n** (n = 12,[19] 14, 16) were corroborated in CD_2Cl_2 solution by NMR spectroscopy at 298 K and are characterised by C_1 symmetry, pairs of alkene ^{1}H resonances with large $^3J_{HH}$ coupling of 15 Hz (CH=CHAr′, δ 7.81–8.05; CH=CHAr′, δ 6.95–7.01), and ^{103}Rh coupled alkyne ^{13}C resonances

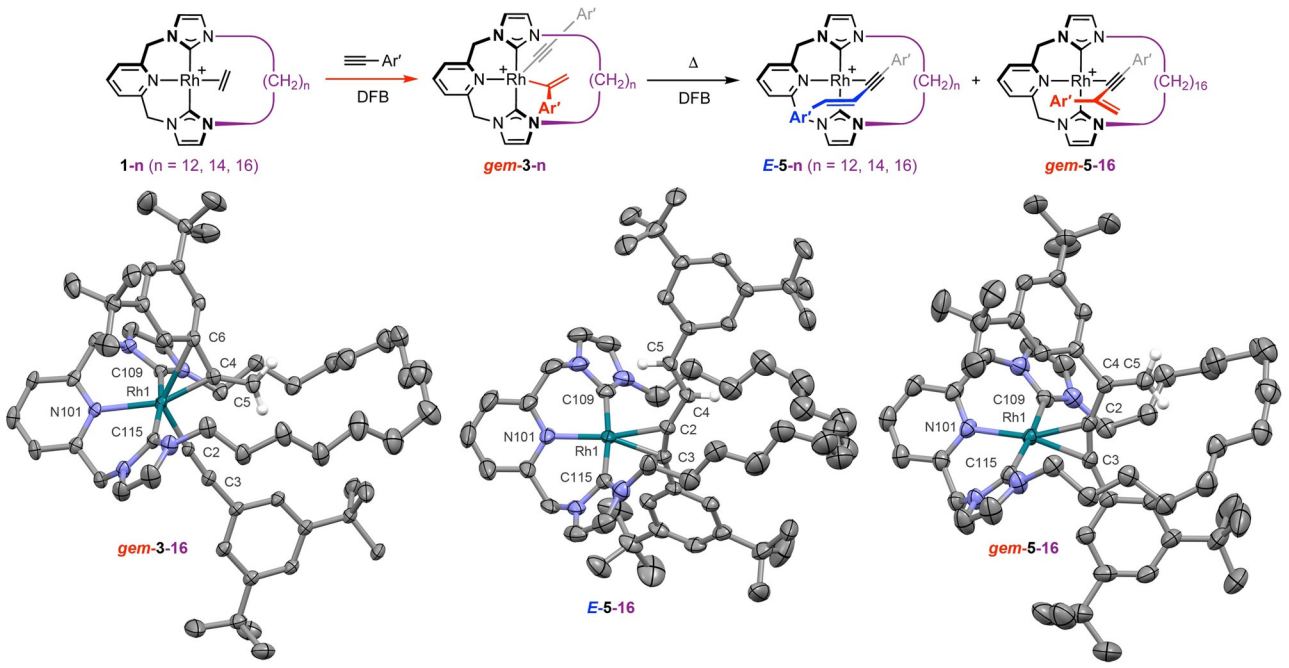

Figure 4. Reactions of **1-n** with HC≡CAr′. Solid-state structures of ***gem*-3-16**, ***E*-5-16** and ***gem*-5-16**: thermal ellipsoids drawn at 30%, 50% and 50% probability, respectively; anions, solvent molecules, minor disordered components (2×*t*Bu and methylene chain, ***E*-5-16**; 1×*t*Bu, ***gem*-5-16**), and most hydrogen atoms omitted for clarity. Selected bond lengths (Å) and angles (deg): ***gem*-3-16**: Rh1-C2, 1.920(5); C2-C3, 1.212(7); Rh1-C2-C3, 171.0(4); Rh1-C4, 1.971(5); C4-C5, 1.328(8); Rh1-C4-C5, 140.2(4); C2-Rh1-C4, 91.6(2); Rh1-C6, 2.508(5); Rh1-N101, 2.232(4); Rh1-C109, 2.068(5); Rh1-C115, 2.072(5); ***E*-5-16**: Rh1-Cnt(C2,C3), 1.996(2); C2-C3, 1.265(4); C2-C4, 1.426(4); C4-C5, 1.340(4); C2-C4-C5, 123.9(3); Rh1-N101, 2.118(3); Rh1-C109, 2.053(4); Rh1-C115, 2.035(3); N101-Rh1-Cnt(C2,C3), 175.25(13); py-Rh-C≡C twist, 35.7(2); ***gem*-5-16**: Rh1-Cnt(C2,C3), 1.990(2); C2-C3, 1.255(4); C2-C4, 1.442(3); C4-C5, 1.334(4); C2-C4-C5, 120.6(2); Rh1-N101, 2.121(2); Rh1-C109, 2.061(2); Rh1-C115, 2.059(3); N101-Rh1-Cnt(C2,C3), 176.98(7); py-Rh-C≡C twist, 31.7(2).

(C≡CAr′, δ 88.9–92.3, $^{1}J_{RhC}$ = 14 Hz; C≡CAr′, δ 83.6–84.0, $^{1}J_{RhC}$ = 13–14 Hz). In addition to verifying the interpenetrated coordination of the enyne, the solid-state structures of ***E*-5-12** and ***E*-5-16** are notable for shorter Rh1-Cnt(C2,C3) and longer C2-C3 contacts [1.981(3)–1.996(2) and 1.255(4)–1.265 Å, respectively] compared to the alkyl *E*-enyne congeners ***E*-4** [2.006(3)–2.040(14) and 1.22(3)–1.245(6) Å, respectively]. The formulation of ***gem*-5-16** was likewise confirmed, with the most pertinent spectroscopic marker the geminal alkene ^{1}H resonances at δ 5.73 and 6.13 [δ(RhC=CH$_2$) 122.0]. There is no statistically significant difference in metal-alkyne contact for the regioisomers [***gem*-5-16**, 1.990(2) Å; ***E*-5-16**, 1.996(2) Å].

Summary and perspectives

The terminal alkyne homocoupling reactions promoted by [Rh(CNC-n)(C$_2$H$_4$)][BAr$^F_4$] (**1-n**; n = 12, 14, 16) discussed herein showcase a uncommon approach for tuning the organometallic reactivity of pincer complexes.[5] In particular, through comparison to the acyclic homologue [Rh(CNC-Me)(C$_2$H$_4$)][BAr$^F_4$] (**1-Me**) and systematic variation of the wingtip linker length, we have been able to deconvolute the impact of the macrocyclic composition from the donor properties of the ligand, with the latter verified by spectroscopic analysis of rhodium(I) carbonyl derivatives (**7**).

The reactions of **1** with alkynes can be reconciled by a hydrometallation mechanism, which bifurcates to afford head-to-head or head-to-tail homocoupling products depending on the regiochemical outcome of 1,2-migratory insertion reactions of rhodium(III) alkynyl hydride derivatives (Scheme 4). This step is selectivity determining for **1-Me** and consequently principally controlled by the *electronic and steric characteristics of the Rh(CNC) core*. For instance, whilst rhodium(III) alkynyl *gem*-alkenyls are formed with HC≡CAr′, the head-to-tail pathway is disfavoured for HC≡C*t*Bu as a consequence of steric buttressing between the pincer backbone and the *tert*-butyl substituent of the π-bound alkyne leading to rhodium(III) alkynyl *E*-alkenyl derivatives.[20] Conjugated 1,3-enynes are produced by C–C bond reductive elimination, *but this step is encumbered when performed through the annulus of macrocyclic CNC ligands*. For the homocoupling of HC≡C*t*Bu, *E*-*t*BuC≡CCH=CH*t*Bu

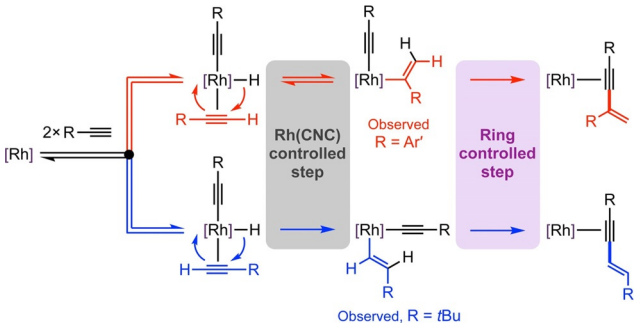

Scheme 4. Overview of terminal alkyne homocoupling reactions promoted by [Rh] = Rh(CNC)$^+$ pincer complexes.

is produced via direct reductive elimination from the corresponding rhodium(III) alkynyl *E*-alkenyl derivatives ***E*-2-n** with increasing efficacy as the ring is expanded. In contrast, direct reductive elimination of Ar′C≡CC(=CH_2)Ar′ from the corresponding rhodium(III) alkynyl *gem*-alkenyl derivatives ***gem*-3-n** is encumbered relative to β-H abstraction and production of *E*-Ar′C≡CCH=CHAr′. Indeed, whilst **1-Me** is a highly effective pre-catalyst for the homocoupling of HC≡CAr′ into Ar′C≡CC-(=CH_2)Ar′ (TOF = 26 h^{-1} in DFB at 298 K), it is only with the hexadecamethylene-based CNC-16 that the two processes are competitive.

Attenuation of the reductive elimination step in terminal alkyne homocoupling reactions is useful from a mechanistic perspective, enabling otherwise fleeting rhodium(III) alkynyl alkenyl derivatives to be isolated (*e.g.* ***E*-2-12**, ***gem*-3-12**, ***gem*-3-14**, ***gem*-3-16**) or spectroscopically characterised *in situ* (*e.g.* ***E*-2-14**, ***E*-2-16**). In terms of practical applications, the net organic transformation is of prospective interest as an "active metal template" method for the construction of mechanically interlocked hydrocarbon molecules.[27] However given the importance of C–C bond coupling reactions in organic and organometallic chemistry, the ability to enforce a change in regioselectivity through use of a macrocyclic ligand has potentially more generalisable practical applications.

Supporting information

Experimental procedures, characterisation data, full details of kinetic measurements, and primary NMR data. Deposition Numbers 2010968, 2010969, 2010970, 2010971, 2010972, 2010973, 2010974, 2010975, 2010976, 2010977, 2010978, 2010979, 2010980, 2010981, 2010982, and 2010983 contain the supplementary crystallographic data for this paper. These data are provided free of charge by the joint Cambridge Crystallographic Data Centre and Fachinformationszentrum Karlsruhe Access Structures service www.ccdc.cam.ac.uk/structures.

Acknowledgements

We thank the European Research Council (ERC, grant agreement 637313; C.M.S., M.R.G., A.B.C.), University of Warwick (R.E.A.), and Royal Society (UF100592, UF150675, A.B.C.) for financial support. High resolution mass-spectrometry data were collected using instruments purchased through support from Advantage West Midlands and the European Regional Development Fund. Crystallographic data for ***E*-4-12**, **6-14** and **6-16** were collected using a diffractometer purchased through support from Advantage West Midlands and the European Regional Development Fund. All other crystallographic data were collected using an instrument that received funding from the ERC under the European Union's Horizon 2020 research and innovation programme (grant agreement 637313).

Conflict of interest

The authors declare no conflict of interest.

Keywords: pincer complexes · macrocyclic ligands · terminal alkyne dimerisation · C–C coupling · enynes

[1] Q. Liang, K. Hayashi, D. Song, *ACS Catal.* **2020**, *10*, 4895–4905; B. M. Trost, J. T. Masters, *Chem. Soc. Rev.* **2016**, *45*, 2212–2238; Y. Zhou, Y. Zhang, J. Wang, *Org. Biomol. Chem.* **2016**, *14*, 6638–6650; M. Nishiura, *J. Mol. Catal. A: Chem.* **2004**, *213*, 101–106.

[2] B. M. Trost, *Angew. Chem. Int. Ed. Engl.* **1995**, *34*, 259–281; *Angew. Chem.* **1995**, *107*, 285–307; B. M. Trost, *Science* **1991**, *254*, 1471–1477.

[3] J. Liu, J. W. Y. Lam, B. Z. Tang, *Chem. Rev.* **2009**, *109*, 5799–5867; K. Ogata, H. Murayama, J. Sugasawa, N. Suzuki, S.-I. Fukuzawa, *J. Am. Chem. Soc.* **2009**, *131*, 3176–3177; M. V. Jiménez, E. Sola, F. J. Lahoz, L. A. Oro, *Organometallics* **2005**, *24*, 2722–2729; J. Wang, A. K. Dash, M. Kapon, J.-C. Berthet, M. Ephritikhine, M. S. Eisen, *Chem. Eur. J.* **2002**, *8*, 5384–5396; A. Haskel, J. Q. Wang, T. Straub, T. G. Neyroud, M. S. Eisen, *J. Am. Chem. Soc.* **1999**, *121*, 3025–3034; T. Straub, A. Haskel, M. S. Eisen, *J. Am. Chem. Soc.* **1995**, *117*, 6364–6365; M. Ishikawa, J. Ohshita, Y. Ito, A. Minato, *J. Chem. Soc. Chem. Commun.* **1988**, 804–805; S. Saito, Y. Yamamoto, *Chem. Rev.* **2000**, *100*, 2901–2916; P. Siemsen, R. Livingston, F. Diederich, *Angew. Chem. Int. Ed.* **2000**, *39*, 2632–2657; *Angew. Chem.* **2000**, *112*, 2740–2767; L. Leroyer, V. Maraval, R. Chauvin, *Chem. Rev.* **2012**, *112*, 1310–1343.

[4] M. Schäfer, J. Wolf, H. Werner, *Dalton Trans.* **2005**, *34*, 1468–1481; H. Werner, M. Schäfer, J. Wolf, K. Peters, H. G. von Schnering, *Angew. Chem. Int. Ed. Engl.* **1995**, *34*, 191–194; *Angew. Chem.* **1995**, *107*, 213–215.

[5] E. Peris, R. H. Crabtree, *Chem. Soc. Rev.* **2018**, *47*, 1959–1968.

[6] *Pincer Compounds: Chemistry and Applications* (Ed.: D. Morales-Morales), Elsevier, **2018**; R. E. Andrew, L. González-Sebastián, A. B. Chaplin, *Dalton Trans.* **2016**, *45*, 1299–1305; *The Privileged Pincer-Metal Platform: Coordination Chemistry & Applications* (Eds.: G. van Koten, R. A. Gossage); *Topics in Organometallic Chemistry, Vol. 40: Organometallic Pincer Chemistry* (Eds.: G. van Koten, D. Milstein), Springer, **2013**; M. Albrecht, M. M. Lindner, *Dalton Trans.* **2011**, *40*, 8733–8744; J. I. van der Vlugt, J. N. H. Reek, *Angew. Chem. Int. Ed.* **2009**, *48*, 8832–8846; *Angew. Chem.* **2009**, *121*, 8990–9004; D. Benito-Garagorri, K. Kirchner, *Acc. Chem. Res.* **2008**, *41*, 201–213; M. E. van der Boom, D. Milstein, *Chem. Rev.* **2003**, *103*, 1759–1792; M. Albrecht, G. van Koten, *Angew. Chem. Int. Ed.* **2001**, *40*, 3750–3781; *Angew. Chem.* **2001**, *113*, 3866–3898.

[7] G. Kleinhans, G. Guisado-Barrios, D. C. Liles, G. Bertrand, D. I. Bezuidenhout, *Chem. Commun.* **2016**, *52*, 3504–3507.

[8] W. Weng, C. Guo, R. Çelenligil-Çetin, B. M. Foxman, O. V. Ozerov, *Chem. Commun.* **2006**, *254*, 197–199.

[9] O. Rivada-Wheelaghan, S. Chakraborty, L. J. W. Shimon, Y. Ben-David, D. Milstein, *Angew. Chem. Int. Ed.* **2016**, *55*, 6942–6945; *Angew. Chem.* **2016**, *128*, 7056–7059.

[10] M. Galiana-Cameo, M. Borraz, Y. Zelenkova, V. Passarelli, F. J. Lahoz, J. J. Pérez-Torrente, L. A. Oro, A. Di Giuseppe, R. Castarlenas, *Chem. Eur. J.* **2020**, *26*, 9598–9608; A. M. Geer, A. Julian, J. A. López, M. A. Ciriano, C. Tejel, *Chem. Eur. J.* **2018**, *24*, 17545–17556; L. Rubio-Pérez, R. Azpíroz, A. Di Giuseppe, V. Polo, R. Castarlenas, J. J. Pérez-Torrente, L. A. Oro, *Chem. Eur. J.* **2013**, *19*, 15304–15314; H.-D. Xu, R.-W. Zhang, X. Li, S. Huang, W. Tang, W.-H. Hu, *Org. Lett.* **2013**, *15*, 840–843; T. Katagiri, H. Tsurugi, T. Satoh, M. Miura, *Chem. Commun.* **2008**, 3405–3407; C.-C. Lee, Y.-C. Lin, Y.-H. Liu, Y. Wang, *Organometallics* **2005**, *24*, 136–143; W. T. Boese, A. S. Goldman, *Organometallics* **1991**, *10*, 782–786; J. Ohshita, K. Furumori, A. Matsuguchi, M. Ishikawa, *J. Org. Chem.* **1990**, *55*, 3277–3280; L. Carlton, G. Read, *J. Chem. Soc. Perkin Trans. 1* **1978**, 1631–1633; S. Yoshikawa, J. Kiji, J. Furukawa, *Makromol. Chem.* **1977**, *178*, 1077–1087; H. Singer, G. Wilkinson, *J. Chem. Soc. A* **1968**, 849–853.

[11] M. Schäfer, J. Wolf, H. Werner, *Organometallics* **2004**, *23*, 5713–5728; I. P. Kovalev, K. V. Yevdakov, Y. A. Strelenko, M. G. Vinogradov, G. I. Nikishin, *J. Organomet. Chem.* **1990**, *386*, 139–146.

[12] C. J. Pell, O. V. Ozerov, *ACS Catal.* **2014**, *4*, 3470–3480.

[13] N. Gorgas, B. Stöger, L. F. Veiros, K. Kirchner, *ACS Catal.* **2018**, *8*, 7973–7982; N. Gorgas, L. G. Alves, B. Stöger, A. M. Martins, L. F. Veiros, K. Kirchner, *J. Am. Chem. Soc.* **2017**, *139*, 8130–8133.

[14] R. Ghosh, X. Zhang, P. Achord, T. J. Emge, K. Krogh-Jespersen, A. S. Goldman, *J. Am. Chem. Soc.* **2007**, *129*, 853–866.

[15] M. R. Gyton, T. M. Hood, A. B. Chaplin, *Dalton Trans.* **2019**, *48*, 2877 – 2880; J. M. Lynam, *Chem. Eur. J.* **2010**, *16*, 8238 – 8247; H. Werner, *Coord. Chem. Rev.* **2004**, *248*, 1693 – 1702.
[16] M. R. Gyton, A. E. Kynman, B. Leforestier, A. Gallo, J. R. Lewandowski, A. B. Chaplin, *Dalton Trans.* **2020**, *49*, 5791 – 5793.
[17] M. R. Gyton, B. Leforestier, A. B. Chaplin, *Organometallics* **2018**, *37*, 3963 – 3971; S. L. Apps, R. E. Alflatt, B. Leforestier, C. M. Storey, A. B. Chaplin, *Polyhedron* **2018**, *143*, 57 – 61; L. González-Sebastián, A. B. Chaplin, *Inorg. Chim. Acta* **2017**, *460*, 22 – 28; R. E. Andrew, C. M. Storey, A. B. Chaplin, *Dalton Trans.* **2016**, *45*, 8937 – 8944; R. E. Andrew, D. W. Ferdani, C. A. Ohlin, A. B. Chaplin, *Organometallics* **2015**, *34*, 913 – 917; R. E. Andrew, A. B. Chaplin, *Inorg. Chem.* **2015**, *54*, 312 – 322.
[18] R. E. Andrew, A. B. Chaplin, *Dalton Trans.* **2014**, *43*, 1413 – 1423.
[19] C. M. Storey, M. R. Gyton, R. E. Andrew, A. B. Chaplin, *Angew. Chem. Int. Ed.* **2018**, *57*, 12003 – 12006; *Angew. Chem.* **2018**, *130*, 12179 – 12182.
[20] C. M. Storey, A. Kalpokas, M. R. Gyton, T. Krämer, A. B. Chaplin, *Chem. Sci.* **2020**, *11*, 2051 – 2057.
[21] S. D. Pike, M. R. Crimmin, A. B. Chaplin, *Chem. Commun.* **2017**, *53*, 3615 – 3633.
[22] A. J. Martínez-Martínez, B. E. Tegner, A. I. McKay, A. J. Bukvic, N. H. Rees, G. J. Tizzard, S. J. Coles, M. R. Warren, S. A. Macgregor, A. S. Weller, *J. Am. Chem. Soc.* **2018**, *140*, 14958 – 14970; R. C. Knighton, J. Emerson-King, J. P. Rourke, C. A. Ohlin, A. B. Chaplin, *Chem. Eur. J.* **2018**, *24*, 4927 – 4938; J. Campos, E. Carmona, *Organometallics* **2015**, *34*, 2212 – 2221; P. Ren, S. D. Pike, I. Pernik, A. S. Weller, M. C. Willis, *Organometallics* **2015**, *34*, 711 – 723; T. Wang, J.-L. Niu, S.-L. Liu, J.-J. Huang, J.-F. Gong, M.-P. Song, *Adv. Synth. Catal.* **2013**, *355*, 927 – 937; B. K. Corkey, F. L. Taw, R. G. Bergman, M. Brookhart, *Polyhedron* **2004**, *23*, 2943 – 2954; F. L. Taw, H. Mellows, P. S. White, F. J. Hollander, R. G. Bergman, M. Brookhart, D. M. Heinekey, *J. Am. Chem. Soc.* **2002**, *124*, 5100 – 5108.
[23] Heating ***E*-2-12** with excess HC≡C*t*Bu resulted in formation of [Rh(CNC-12)(*E*-*t*BuCH=CC≡C*t*Bu)(*E*-CH=CH*t*Bu)][BAr^F_4]. Further details and the solid-state structure of this rhodium(III) derivative are provided in the ESI.
[24] Indeed, this assertion is supported by a computational analysis of homocoupling reactions of HC≡CPh and HC≡C*t*Bu catalysed by **1-Me**. See ref. [20].
[25] D. J. Nielsen, K. J. Cavell, B. W. Skelton, A. H. White, *Inorg. Chim. Acta* **2002**, *327*, 116 – 125.
[26] T. M. Hood, M. R. Gyton, A. B. Chaplin, *Dalton Trans.* **2020**, *49*, 2077 – 2086; B. Leforestier, M. R. Gyton, A. B. Chaplin, *Dalton Trans.* **2020**, *49*, 2087 – 2101; G. L. Parker, S. Lau, B. Leforestier, A. B. Chaplin, *Eur. J. Inorg. Chem.* **2019**, 3791 – 3798; J. J. Davidson, J. C. DeMott, C. Douvris, C. M. Fafard, N. Bhuvanesh, C.-H. Chen, D. E. Herbert, C.-I. Lee, B. J. McCulloch, B. M. Foxman, O. V. Ozerov, *Inorg. Chem.* **2015**, *54*, 2916 – 2935.
[27] M. Denis, S. M. Goldup, *Nat. Rev. Chem.* **2017**, *1*, 0061; J. E. M. Lewis, P. D. Beer, S. J. Loeb, S. M. Goldup, *Chem. Soc. Rev.* **2017**, *46*, 2577 – 2591; J. D. Crowley, S. M. Goldup, A.-L. Lee, D. A. Leigh, R. T. McBurney, *Chem. Soc. Rev.* **2009**, *38*, 1530 – 1541.

Manuscript received: June 20, 2020
Revised manuscript received: July 15, 2020
Accepted manuscript online: July 17, 2020
Version of record online: October 12, 2020